

Received October 15, 2017, accepted November 20, 2017, date of publication November 27, 2017,  
 date of current version February 14, 2018.

Digital Object Identifier 10.1109/ACCESS.2017.2777899

# TDA-MAC: TDMA Without Clock Synchronization in Underwater Acoustic Networks

**NILS MOROZS<sup>ID</sup>, (Member, IEEE), PAUL MITCHELL<sup>ID</sup>, (Senior Member, IEEE),  
 AND YURIY V. ZAKHAROV<sup>ID</sup>, (Senior Member, IEEE)**

Department of Electronic Engineering, University of York, York YO10 5DD, U.K.

Corresponding author: Nils Morozs (nils.morozs@york.ac.uk)

This work was supported by the U.K. Engineering and Physical Sciences Research Council through the USMART Project under Grant EP/P017975/1.

**ABSTRACT** This paper investigates the application of underwater acoustic sensor networks for large scale monitoring of the ocean environment. The low propagation speed of acoustic signals presents a fundamental challenge in coordinating the access to the shared communication medium in such networks. In this paper, we propose two medium access control (MAC) protocols, namely, Transmit Delay Allocation MAC (TDA-MAC) and Accelerated TDA-MAC, that are capable of providing time division multiple access (TDMA) to sensor nodes without the need for centralized clock synchronization. A comprehensive simulation study of a network deployed on the sea bed shows that the proposed protocols are capable of closely matching the throughput and packet delay performance of ideal synchronized TDMA. The TDA-MAC protocols also significantly outperform T-Lohi, a classical contention-based MAC protocol for underwater acoustic networks, in terms of network throughput and, in many cases, end-to-end packet delay. Furthermore, the assumption of no clock synchronization among different devices in the network is a major advantage of TDA-MAC over other TDMA-based MAC protocols in the literature. Therefore, it is a feasible networking solution for real-world underwater sensor network deployments.

**INDEX TERMS** Medium access control, TDMA, underwater acoustic network, wireless sensor network.

## I. INTRODUCTION

The use of wireless sensor networks for remote monitoring of the ocean environment is becoming an increasingly popular research subject, owing to the modern developments in underwater acoustic modem technologies [1], [2]. In contrast with terrestrial wireless communication systems, underwater radio propagation is severely limited in range due to high absorption of electromagnetic (EM) waves in seawater, while optical communications suffer from both high absorption and optical scattering [3]. Acoustic waves are the preferred practical medium of communication in the underwater environment; they exhibit significantly better propagation characteristics compared with EM waves. However, the performance of acoustic communication systems is fundamentally limited by the low sound propagation speed, approximately 1500 m/s in water, and by the small available bandwidth with carrier frequencies typically in tens of kHz, or lower for long range transmissions [2], [3].

The long propagation delays of acoustic signals present a significant challenge in Medium Access Control (MAC), i.e. coordinating transmissions of multiple acoustic

communication nodes potentially spaced kilometers apart from one another. In this paper, we consider the problem of Time Division Multiple Access (TDMA), where data packets from multiple nodes are required to arrive at an intended receiver without overlapping in time, e.g. [4]–[6]. TDMA is a more flexible multiple access technology compared with Frequency Division Multiple Access (FDMA) [7] and Code Division Multiple Access (CDMA) [8], because it can provide a variable number of orthogonal channels without any adjustments to the hardware, and allocate variable data rates by adjusting the number of time slots assigned to a particular node [2]. However, TDMA typically requires centralized coordination and clock synchronization among different nodes for scheduling their transmissions appropriately. As an alternative to deterministic schedule-based TDMA methods, communication networks often use contention-based MAC protocols where nodes access a shared channel randomly on demand, based on a particular set of rules [9]. However, most conventional contention-based MAC protocols are highly inefficient in the underwater acoustic environment. For example, channel reservation based protocols waste a

large part of channel capacity while the nodes are waiting for control signals to propagate through the slow acoustic medium to establish a communication link, e.g. Request-to-Send (RTS), Clear-to-Send (CTS), acknowledgements etc. These waiting times result in significant loss of throughput and poor channel utilization [2], [10], [11]. Furthermore, Carrier Sense Multiple Access (CSMA) techniques, where nodes are “listening” for the presence of other packets on the shared channel before transmitting, are also inefficient in underwater acoustic networks (UANs). In order for UAN nodes to accurately detect when the channel is free using carrier sensing, excessive guard intervals are required to compensate for the long propagation delays [2]. Such a dramatic change in the operating conditions, compared with terrestrial radio systems, presents the need for the design of MAC protocols dedicated specifically to UANs.

A large proportion of the well-established research on MAC in UANs has focused on improving contention-based protocols that involve control signaling for reserving the acoustic channel, e.g. [10]–[13]. One of the well-known MAC protocols designed for UANs is T-Lohi [12]. It is a distributed MAC protocol where network nodes resolve contention for the communication resources in a distributed and energy-efficient way by using short contention tones and pre-defined waiting times. However, at higher traffic loads, when many nodes contend for the resources, the reservation period, i.e. the time it takes for one node to win the contention, is likely to significantly exceed the duration of the actual data transmission, which results in low channel utilization. In another example, Liao and Huang [13] propose SF-MAC, a Spatially Fair MAC protocol for UANs. It is an RTS/CTS based MAC protocol which resolves spatial unfairness in contention-based MAC, i.e. when the nodes closer to the receiver are more likely to reserve the channel due to significantly smaller propagation delays. Noh *et al.* [11] propose the Delay-aware Opportunistic Transmission Scheduling (DOTS) protocol which leverages locally obtained propagation delay information at every node to opportunistically schedule concurrent transmissions while reducing the chance of collisions. They show that the DOTS protocol provides stable throughput performance and fair channel access even with node mobility. Another well-known example in the literature is the Slotted Floor Acquisition Multiple Access (Slotted FAMA) protocol proposed by Molins and Stojanovic [10], which involves both carrier sensing and a slotted timing structure for control signaling between a transmitter and a receiver, which provides significant energy savings compared with the original FAMA protocol [14] due to the decreased length of RTS and CTS packets. However, despite the efficiency of the contention-based MAC protocols designed for UANs, compared with their terrestrial radio counterparts, their throughput performance is fundamentally limited by the long waiting times due to slowly propagating control signals.

A significantly more efficient class of MAC protocols in terms of channel throughput are the schedule-based TDMA schemes. There, the nodes are scheduled to transmit their

data packets in particular time slots such that the packets arrive at the intended receiver without collisions, e.g. [5], [6]. TDMA schemes do not involve contention for communication resources and, therefore, remove the need for control signaling in order to establish collision-free links. This allows TDMA-based MAC protocols to achieve high throughput by efficiently scheduling transmissions from nodes in a way that results in a stream of data packets and short guard intervals at the intended receivers. The drawback of TDMA approaches is their need for clock synchronization across different nodes, which is a challenging task in UANs due to long propagation delays, noisy time-varying multipath channels, and the signaling overhead that is not negligible compared with terrestrial radio systems [2], [15]. The use of chip-scale atomic clocks [16] is an alternative way of providing an accurate synchronized time reference to the network nodes for long periods of time, but they are not feasible in many deployment scenarios, in particular due to their excessive cost, higher power consumption and ageing [17], [18].

There are many research publications on the design of such collision-free TDMA transmission schedules for various network topologies and types of traffic. For example, Lmai *et al.* [6] derive transmission schedules for ad hoc UANs with linear topologies both for unicast and broadcast traffic, that maximize the network throughput. In [19] the same authors derive throughput-maximizing schedules for multi-hop grid networks, which exploit long propagation delays by allowing multiple simultaneous transmissions. A well-known schedule-based MAC protocol designed for UANs is the Staggered TDMA Underwater MAC Protocol (STUMP) [5]. It offsets the TDMA frame timing at every node based on knowledge of their propagation delays and, thus, achieves high channel utilization. Kredo II *et al.* [5] also demonstrate that STUMP achieves adequate performance even with errors in node synchronization and the propagation delay estimates. Yackowski and Shen [4] propose the UW-FLASHR algorithm that allows the nodes to dynamically acquire time slots for data transmissions with few collisions, without the need for centralized control, tight clock synchronization or accurate propagation delay estimates. It achieves channel utilization of up to 80%; however, its performance significantly degrades with longer propagation delays and shorter packet durations. For example, with 50 byte long packets, 15 kbps bitrate and a maximum propagation delay of 1 second, the channel utilization of UW-FLASHR drops to approximately 10%.

Many of the proposed collision-free scheduling MAC protocols do not require a precise global time reference; however, their performance tends to visibly deteriorate with loose clock synchronization. To our knowledge, there is no evidence in the literature of TDMA-based protocols that are explicitly designed to operate without the need for any clock synchronization in UANs, i.e. where the timing reference distributed across the network is embedded into the MAC algorithm itself. The purpose of this paper is to propose such a TDMA-based MAC algorithm which can match the

performance of an ideal staggered TDMA scheme, but without the need for clock synchronization across different nodes in the network.

The major contributions presented in this paper are the following:

- We propose a novel centralized MAC algorithm for UANs, Transmit Delay Allocation MAC (TDA-MAC), which is capable of matching the performance of an ideal staggered TDMA protocol, but assumes no clock synchronization among the network nodes.
- The thorough TDA-MAC algorithm specification given in the paper does not assume any pre-existing knowledge of the network topology. It gives details on how TDA-MAC can be implemented on every individual node and how the necessary propagation delay estimates can be obtained and kept up-to-date as part of the proposed MAC algorithm.
- We then introduce an extension to TDA-MAC which enhances its performance and allows it to approach the maximum theoretical throughput performance, at the expense of requiring a dedicated channel or spreading sequence for control packets, even in small networks with short packet durations with respect to the propagation delays. It is referred to as Accelerated TDA-MAC (ATDA-MAC).
- We present results of a detailed simulation study based on a realistic deployment of an acoustic sensor network with 20-100 nodes for seismic monitoring in oil reservoirs. It uses a sound speed profile (SSP) obtained from real data for the North Atlantic Ocean, and the BELLHOP ray tracing program [20] to simulate acoustic ray trajectories and propagation delays.

The rest of the paper is organized as follows: Section II introduces the problem of underwater acoustic sensor networking and its challenges; Section III describes the proposed TDA-MAC and ATDA-MAC protocols; Section IV presents the outcomes of the detailed simulation study; finally, Section V concludes the paper.

## II. UNDERWATER ACOUSTIC SENSOR NETWORKS

This paper focuses on MAC in underwater acoustic sensor networks with tens or even hundreds of communication nodes producing large amounts of interference that must be managed appropriately. In this section, we give an overview of typical UAN architectures used for environmental monitoring applications, discuss the data traffic patterns in such networks, and describe the challenges of underwater acoustic propagation related to networking.

### A. UNDERWATER SENSOR NETWORK ARCHITECTURES

Fig. 1 depicts typical underwater wireless sensor network deployment scenarios for environmental monitoring applications, such as water pollution measurements [21], fish tracking [22], seismic monitoring in oil reservoirs [23], etc. The wireless sensor network approach to ocean monitoring provides significant advantages over the traditional deployment

of wired sensor platforms from dedicated ships, because the former allows flexible long term deployments and eliminates the need for retrieving the sensor nodes from the sea bed in order to collect the data.

Fig. 1a provides a general overview of the types of architectures and links required for ocean monitoring. Sensor nodes that are deployed close to the shore communicate with a base station either directly or via a relay node or other sensor nodes (multi-hop topologies); the base station on the shore can then relay the received data via wired or radio links to the headquarters. In network deployments further away from the shore, a surface buoy may be used to collect the data from the underwater sensor nodes via acoustic signals and then relay that data via radio to the on-shore base station. Alternatively, autonomous underwater vehicles (AUVs) may be deployed as data mules, because they can get closer to the sensor nodes and communicate with them more reliably and at higher data rates, e.g. [24]. In contrast, a common approach in current ocean measurement campaigns is a dedicated shipping expedition, where the sensor nodes are deployed and retrieved manually with the data stored locally on the sensor nodes.

A more specific underwater acoustic sensor network deployment scenario is depicted in Fig. 1b. There, a large number of sensors are deployed on the sea bottom above an oil reservoir for seismic monitoring, either for detecting random seismic events or for continuous monitoring of the deformations in the sea bed [25]. The network topology used in the simulation studies in this paper is based on this oil reservoir seismic monitoring use case, but is generally applicable to a variety of other sea bed environmental monitoring applications.

### B. SENSOR NETWORK TRAFFIC

A classical traffic model that has been used for decades for evaluating the MAC protocol performance in terrestrial networks is the random Poisson traffic model [26]. There, the packet inter-arrival times at every network node are modeled as independent exponentially distributed random events. Although studies have shown that it is often an inaccurate representation of real-world network traffic, e.g. [27], [28], it enables tractable theoretical analysis of network performance and is still extensively used for simulation studies, including many on MAC in UANs, e.g. [12], [13], [29].

We argue that many wireless sensor network applications, particularly for environmental monitoring tasks, do not involve random bursty traffic but rather a periodic data gathering arrangement, where the network is configured such that every node periodically transmits a packet with a sensor reading to a base station or a gateway node, e.g. [30]. For this type of traffic, opportunistic and contention based MAC protocols are inappropriate, since they are typically optimized to deal with unpredictable random traffic patterns. In contrast, collision-free TDMA based MAC protocols are a more relevant solution because they enable highly efficient and well-structured packet reception patterns at the receiver, e.g. [5] [6].

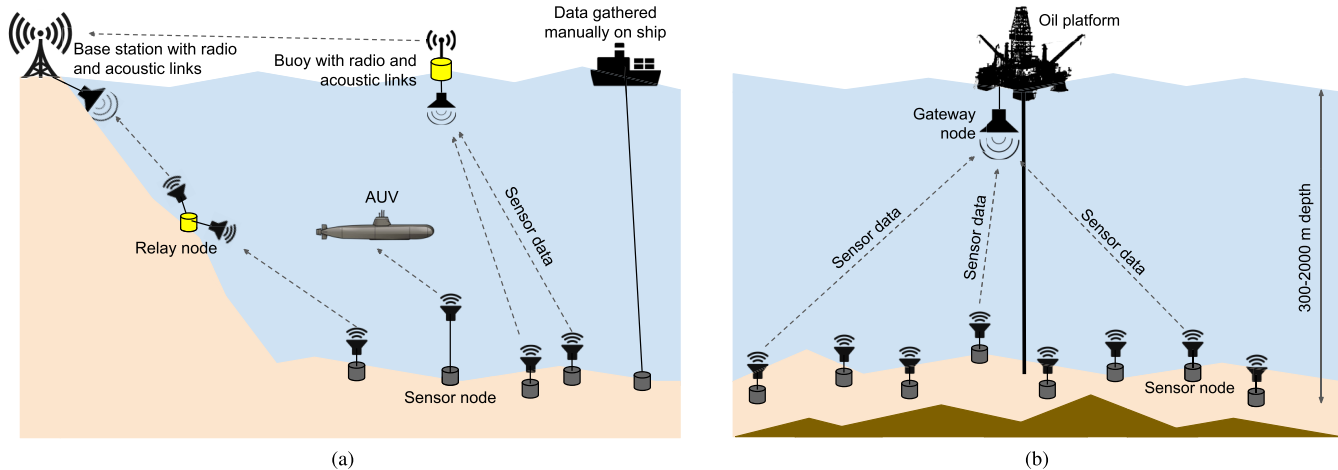


**FIGURE 1.** Applications of underwater acoustic sensor networks. (a) Environmental monitoring. (b) Seismic monitoring in oil reservoirs.

The MAC protocols proposed in this paper are initially designed for periodic data gathering scenarios in underwater acoustic sensor networks, but are then evaluated in scenarios with random bursty traffic conditions, as general TDMA-based MAC protocols.

### C. ACOUSTIC SIGNAL PROPAGATION

The dominant limiting factor affecting the performance of MAC algorithms in underwater acoustic networks is the low sound propagation speed. In contrast with terrestrial radio networks with a propagation speed of  $3 \times 10^8$  m/s, acoustic waves propagate through water at approximately 1500 m/s, i.e. slower by a factor of  $2 \times 10^5$ . For example, if an acoustic link range exceeds 1.5 km, it will take more than 1 second for the signal to propagate across. Furthermore, the sound speed depends on the temperature, pressure and salinity of the water and is, therefore, variable in space and time [31]. Fig. 2 shows an example of a depth-dependent sound speed profile (SSP) derived by Dushaw [32] from the 2009 World Ocean Atlas temperature, pressure and salinity data in summer at (56.5°N, 11.5°W), i.e. in the North Atlantic Ocean off the coast of the UK and Ireland.

The depth-dependent SSP causes refraction of the acoustic waves, which in turn results in curved propagation trajectories as shown in Fig. 3. These plots were obtained using the BELLHOP ray tracing program [20] based on the SSP data shown in Fig. 2b. Firstly, the ray trajectories illustrated in Fig. 3 demonstrate that calculating propagation delays based on a Euclidean distance between two communication nodes, a method often used in UAN MAC research [13], [29], is not always valid, since the signal arriving at the receiver may not travel in a straight line. There also may not be a direct path between two nodes, but only a path reflected off the sea surface or bottom. Secondly, using a single value of the propagation speed could also be inaccurate, e.g. a typical 1500 m/s approximation [12], [13], [29], since the sound speed varies with depth. Furthermore, curved trajectories of the acoustic

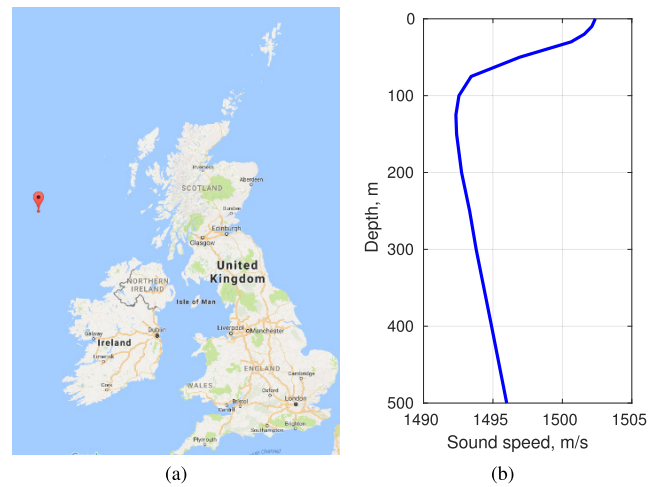


**FIGURE 2.** Example of an SSP in the North Atlantic Ocean based on average summer temperature, pressure and salinity data at (56.5°N, 11.5°W). (a) Google Maps location. (b) Sound speed profile.

waves can result in challenging multipath channel conditions, where several refracted echoes of the same signal arrive at the receiver at different times, in addition to the echoes reflected off the surface and bottom of the sea.

Such a challenging propagation environment, compared with the terrestrial radio environment, presents the need for MAC protocols dedicated to UANs. In the next section we present a centralized MAC protocol designed to tackle the severe propagation delays of acoustic signals and the space-time uncertainty that stems from them, but which does not assume any knowledge of the network topology at the surface base station node (referred to as the gateway node).

### III. TRANSMIT DELAY ALLOCATION MAC

The main principle behind the Transmit Delay Allocation MAC protocol (TDA-MAC) proposed in this section is to achieve a TDMA-like slotted packet reception at the surface

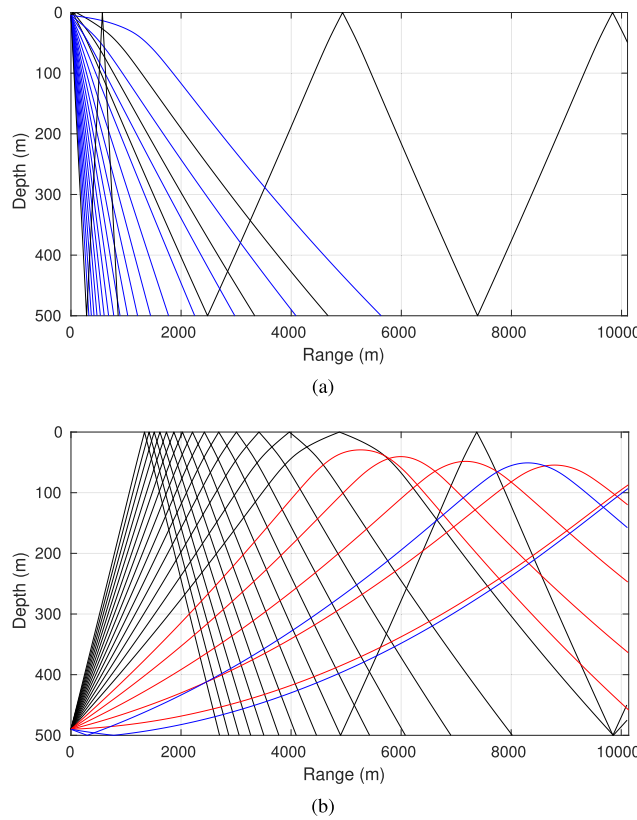


**FIGURE 3.** Acoustic ray trajectories obtained using the BELLHOP simulator. (a) Surface node to sea bottom node propagation (source depth - 5m). (b) Sea bottom node to sea bottom node propagation (source depth - 490m).

gateway node, acting as a base station, without synchronizing the clocks at every wireless sensor node deployed in a UAN, such as those depicted in Fig. 1. This is achieved via the gateway node's ability to estimate the propagation delays to all sensor nodes in the network, as explained in the following subsection.

For the reader's reference, Table 1 contains a list of mathematical terms used in the rest of this section.

**TABLE 1.** List of mathematical terms.

Term	Description
$\tau_p[n]$	Propagation delay between gateway node and $n^{th}$ sensor node
$\tau_{tx}[n]$	Transmit delay allocated to $n^{th}$ sensor node
$\tau_{tx}^*[n]$	Initial hypothetical transmit delay allocated to $n^{th}$ sensor node
$\tau_{min}$	Minimum first node delay
$T_{dp}[n]$	Duration of the $n^{th}$ sensor node's data packet
$T_g[n]$	Duration of the guard interval after the data packet received from $n^{th}$ sensor node
$T_{rp}$	Duration of the data request (REQ) packet
$T_{g,RP}$	Duration of the guard interval after transmitting the REQ packet
$T_{frame}$	Frame duration (interval between two consecutive REQ packets)
$T_{frame,min}$	Smallest possible frame duration
$T_{min,delay}$	Constraint on $T_{frame}$ due to propagation delays
$T_{min,channel}$	Constraint on $T_{frame}$ due to channel capacity
$N$	Number of sensor nodes
$N_{adv}$	Number of data packet slots by which the REQ packet transmission is advanced

#### A. THE TDA-MAC PROTOCOL

First, the propagation delays need to be accurately measured by sequentially exchanging PING packets between the gateway node and every sensor node, as shown in an example with three nodes in Fig. 4. The duration of this process is approximately equal to the average roundtrip delay between the gateway node and the sensor nodes, i.e. typically in the order of several minutes. Note that any small inaccuracies in

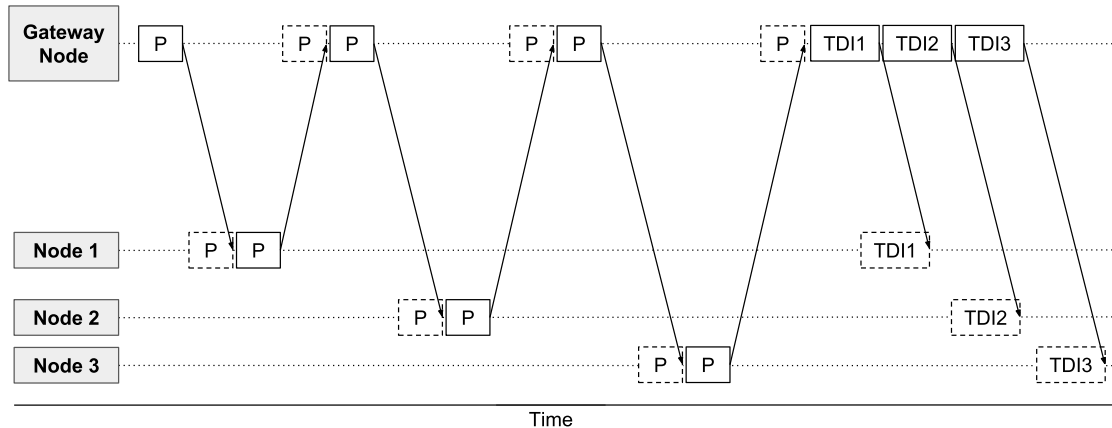


**FIGURE 4.** Setup stage signalling in TDA-MAC, where the gateway node measures all propagation delays and, afterwards, sends a transmit delay instruction packet to every node; P - ping, TDI - transmit delay instruction.

the propagation delay estimates, e.g. due to surface waves and ocean currents causing node displacement, can be accounted for by increasing the guard intervals between consecutively scheduled data packets. Afterwards, a transmit delay instruction (TDI) packet is sent to every sensor node, stating the amount of time it has to wait between receiving a data request (REQ) packet from the gateway node and starting its data transmission. The latter process is depicted in Fig. 5. There, the gateway node transmits a broadcast REQ packet that is received at every node at a different time (due to different propagation delays of acoustic signals). Upon receiving the broadcast REQ packet, any node that has data to transmit, waits a particular amount of time, defined in its transmit delay instruction, and then transmits its data packet.

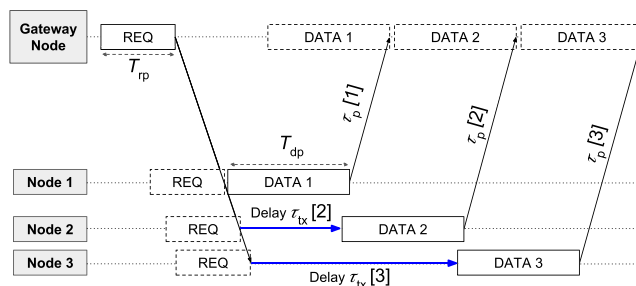


**FIGURE 5.** Packet flow in TDA-MAC; REQ - data request packet.

This process results in a slotted TDMA-like packet reception at the gateway node depicted in Fig. 5 without the need for clock synchronization at the wireless sensor nodes. Afterwards, during the normal operation of the network, i.e. after the initial sequence of PING signals, the gateway node can continuously monitor the accuracy of the estimated propagation delays by measuring the error in the timing of the received data packets. For example, if a data packet from a particular sensor node arrives  $\tau_{\text{error}}$  seconds later or earlier than expected, the propagation delay estimate for this node is off by  $\tau_{\text{error}}/2$ . The gateway node can then transmit updated TDI packets to one or more sensor nodes without the need for another round of PING signal exchanges.

The transmit delay for the  $n^{\text{th}}$  node, where  $n = 1, 2, 3, \dots, N$  is calculated as:

$$\tau_{\text{tx}}[n] = \tau_{\text{tx}}[n-1] + T_{\text{dp}}[n-1] + T_g[n-1] - 2(\tau_p[n] - \tau_p[n-1]), \quad (1)$$

where  $\tau_p[n]$  is the propagation delay from the gateway node to the  $n^{\text{th}}$  sensor node,  $\tau_{\text{tx}}[n]$  is the transmit delay assigned to the  $n^{\text{th}}$  sensor node,  $\tau_{\text{tx}}[1] = 0$ , i.e. the first node starts transmitting its data packet as soon as it receives the REQ packet from the gateway node,  $T_{\text{dp}}[n]$  is the duration of the  $n^{\text{th}}$  node's data packet and  $T_g[n]$  is the guard interval after the  $n^{\text{th}}$  node's data packet reception at the gateway node. The nodes in the  $\tau_{\text{tx}} = (\tau_{\text{tx}}[1], \tau_{\text{tx}}[2], \dots, \tau_{\text{tx}}[N])$  and  $\tau_p = (\tau_p[1], \tau_p[2], \dots, \tau_p[N])$  vectors are sorted from the shortest to the longest propagation delay from the gateway node. Depending on the difference in propagation delays between

two consecutive nodes ( $\tau_p[n] - \tau_p[n-1]$ ), some transmit delays calculated using (1) may be negative. In those cases we set them to zero before continuing to iterate over the rest of the nodes in  $\tau_{\text{tx}}$ , i.e. we place the following constraint on  $\tau_{\text{tx}}[n]$ :

$$\forall n \in [1, N], \quad \tau_{\text{tx}}[n] \geq 0 \quad (2)$$

Another parameter that needs to be established by the gateway node is the regularity (i.e. the period) of the TDMA frames, during which every sensor node gets an opportunity to transmit a data packet. This frame period is specific to any given application depending on how frequently the sensor readings need to be gathered. However, there is a constraint on the minimum frame period that depends on the propagation delays in the network. This constraint is given by:

$$T_{\text{frame}} \geq \max_n \{2 \tau_p[n] + \tau_{\text{tx}}[n] + T_{\text{dp}}[n]\} + T_{\text{rp}}, \quad (3)$$

where  $T_{\text{rp}}$  is the duration of the REQ packet, and  $T_{\text{frame}}$  is the frame period, i.e. the time interval between two consecutive REQ packet transmissions. The above expression states that the gateway node cannot transmit the REQ packet for the next frame before it finishes receiving a data packet from the last sensor node.

**Algorithm 1** TDA-MAC Algorithm Implementation on the Gateway Node (Base Station); TDI - Transmit Delay Instruction, REQ - Data Request Packet

```

1: for every sensor node ( $n = 1, 2, 3, \dots, N$ ) do
2:   Transmit PING packet to  $n^{\text{th}}$  sensor node
3:   Wait for PING packet back from  $n^{\text{th}}$  sensor node
4:   Calculate propagation delay  $\tau_p[n]$  to  $n^{\text{th}}$  sensor node
5: end for
6: Calculate Tx delay  $\tau_{\text{tx}}[n]$  for every  $n$  using (1), under constraint given by (2)
7: Determine the period of TDMA frames under constraint given by (3)
8: Transmit TDI packet to every node sequentially
9: while TDMA slot jitter is below threshold (no collisions) do
10:  Transmit broadcast REQ packet
11:  Receive data packets from sensor nodes in their allocated slots
12:  Measure the errors between expected and actual TDMA slot timing
13:  if TDMA slot jitter is above a threshold then
14:    Adjust propagation delay estimates using the measured timing errors
15:  Go to Step 6
16:  end if
17: end while
```

Algorithm 1 shows the sequence of steps required at the gateway node to control the operation of the TDA-MAC protocol illustrated in Figs. 4 and 5. It takes into account potential errors in TDMA slot timing (jitter) in realistic environments, e.g. if the propagation delays change over time and

the assigned transmit delays need to be adjusted. Algorithm 2 shows the implementation of the proposed protocol at every sensor node. It demonstrates the low complexity and computing requirements of the TDA-MAC implementation on the sensor nodes; they only need to perform three basic reactive operations depending on the type of packet they receive from the gateway node. Most of the intelligence associated with TDA-MAC is implemented on the gateway node. The low algorithm complexity on the sensor node side can become a significant factor in future deployments of large scale sensor networks comprising low cost, low specification nodes, e.g. such as those developed at University of Newcastle, UK [33].

**Algorithm 2** TDA-MAC Algorithm Implementation on a Sensor Node; TDI - Transmit Delay Instruction, REQ - Data Request Packet

- ```

1: if PING packet received from gateway node then
2:   Transmit PING packet back to gateway node
3: end if
4: if TDI packet received from gateway node then
5:   Store transmit delay allocated to this node
6: end if
7: if REQ packet received from gateway node then
8:   Schedule packet transmission with allocated delay
9: end if

```

### B. CHANNEL UTILIZATION OF TDA-MAC

The maximum achievable throughput of the TDA-MAC protocol can be derived by analyzing a generalized version of the timeline shown in Fig. 5. It is given by the following closed form expression:

$$\gamma_{\max} = \frac{\sum_{n=1}^N T_{dp}[n]}{T_{rp} + 2 \min_n \{\tau_p[n]\} + \sum_{n=1}^N (T_{dp}[n] + T_g[n])}, \quad (4)$$

where  $\gamma_{\max}$  is the maximum channel utilization, i.e. network throughput normalized by the channel bitrate. This expression incorporates both the network topology (the shortest roundtrip propagation delay) and the packet and channel characteristics (packet lengths). It shows that TDA-MAC will achieve better network throughput with a higher number of nodes and longer packet lengths, but is also affected by the propagation delays. This analytical prediction of the TDA-MAC network throughput is later compared with the simulation results discussed in Section IV.

Fig. 5 shows that the proposed TDA-MAC algorithm has a channel utilization gap during the initial waiting period between the gateway node transmitting the data request packet and receiving the first data packet from a sensor node. This delay is equal to the round trip time from the gateway node to the sensor node with the shortest propagation delay. Furthermore, Equation (4) shows that the network

throughput achieved by TDA-MAC will decrease if the data packet duration ( $T_{dp}$ ) decreases with respect to the round trip time from the gateway node to the first sensor node  $2 \min_n \{\tau_p[n]\}$ . Fig. 6 illustrates this decrease in channel utilization of TDA-MAC with shorter data packets, compared with the timeline shown in Fig. 5.

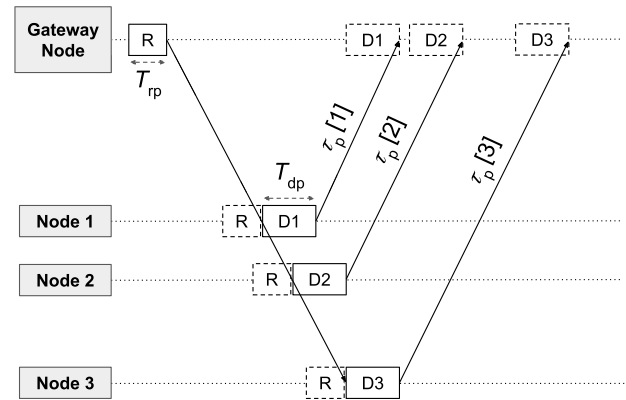


**FIGURE 6.** Gaps in channel utilization using TDA-MAC due to short packet duration and long propagation delays; R - data request (REQ) packet, D - data packet.

In addition to the channel utilization gap due to the roundtrip time from the gateway node and the first sensor node, Fig. 6 depicts another limitation on the throughput of TDA-MAC, that is not accounted for by Equation (4). Despite the fact that all three depicted nodes transmit data packets as soon as they receive the REQ packet, i.e. their assigned Tx delays are all zero, there are now gaps between the reception of successive data packets at the gateway node that further reduce the overall channel utilization. The presence of these gaps between packets depends on the distribution of the propagation delays in the network. They arise under the following condition:

$$T_{dp}[n] + T_g[n] < 2(\tau_p[n+1] - \tau_p[n]), \quad (5)$$

i.e. if the data packet slot is shorter than double the difference in propagation delays from the gateway node to two consecutively scheduled sensor nodes. It includes the factor of two because it takes  $\tau_p[n+1] - \tau_p[n]$  longer both for the REQ packet to reach node  $n+1$ , and for the data packet to travel back from node  $n+1$  to the gateway node.

A more accurate mathematical prediction of the network throughput, that takes into account the potential gaps between consecutive data packets, is given by the following equation:

$$\gamma_{\max} = \frac{\sum_{n=1}^N T_{dp}[n]}{\max_n \{2 \tau_p[n] + \tau_{tx}[n] + T_{dp}[n]\} + T_{rp}}, \quad (6)$$

which is a ratio between the total duration of the data packets received from all nodes and the minimum TDA-MAC frame duration given by (3). However, this formula requires the knowledge of the assigned transmit delays  $\tau_{tx}$ , which are

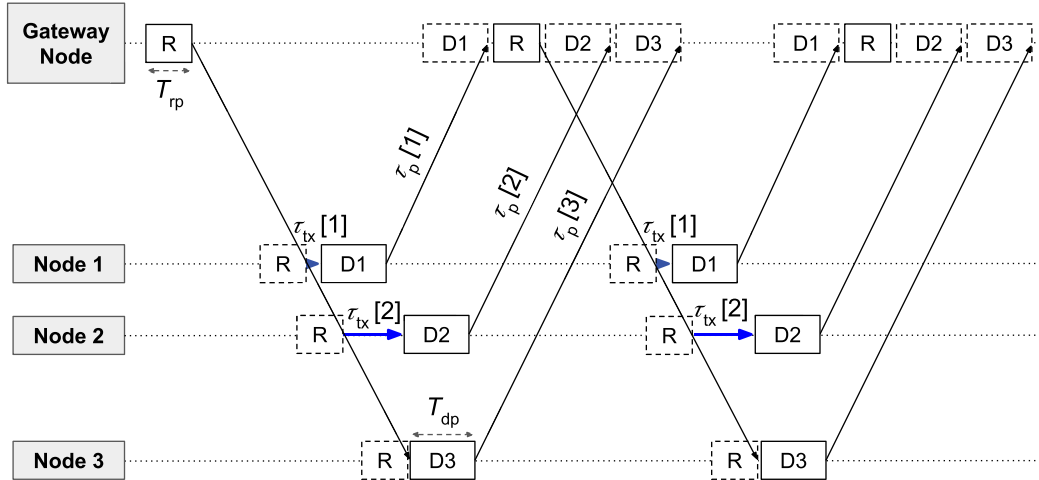


**FIGURE 7.** Packet flow in Accelerated TDA-MAC, where the broadcast REQ signal is transmitted before the end of the current set of data packet slots to increase the channel utilization; R - data request (REQ) packet, D - data packet,  $\tau_{tx}[n]$  - Tx delay.

specific to the TDA-MAC protocol, whereas the analytical network throughput prediction given by (4) uses only the general parameters of the deployment scenario - propagation delays and packet durations.

### C. ACCELERATED TDA-MAC

In order to overcome the channel utilization limitations of TDA-MAC described above, we propose an extension to our algorithm - Accelerated TDA-MAC (ATDA-MAC). Instead of waiting to receive the data packets from all sensor nodes before transmitting the next broadcast REQ packet, in ATDA-MAC, the gateway node schedules the REQ packet transmission before the end of the current frame, as shown in Fig. 7. There, the REQ packet transmission is scheduled before data packet reception from nodes 2 and 3. As a result the channel underutilization due to the propagation delay distribution is alleviated, because the packet reception from other nodes is used to fill the airtime that would be unused by TDA-MAC.

The channel throughput in the simple scenario in Fig. 7 could be further improved by scheduling the REQ packet transmission before the node 1 data packet slot. In this way all three data packets are scheduled to be received during the roundtrip delay between gateway node and node 1, thus achieving near-full channel utilization. However, the additional requirement of ATDA-MAC would be a dedicated channel or spreading sequence for the REQ packets, because, unlike the original TDA-MAC scheme proposed in Subsection III-A, the REQ packets received at the sensor nodes will collide with the interfering data packets transmitted from other sensor nodes to the gateway node. More generally, the broadcast REQ signals need to be resilient to interference from the data packets. Such signals can also be a particular unique spread spectrum waveform, since their content is always the same. The entire purpose of the REQ signals is to notify every sensor node that it can transmit a data packet

and to give it a reference time to start counting its assigned Tx delay.

The rest of this section gives the mathematical derivation of the frame interval  $T_{\text{frame}}$  and the vector of Tx delays assigned to every node  $\tau_{tx}$ , such that the network exhibits the ATDA-MAC packet structure depicted in Fig. 7.

### D. ATDA-MAC: SCHEDULING THE BROADCAST REQ PACKET

First, after measuring the propagation delays to all sensor nodes, the gateway node has to establish how many data packet slots in advance it can schedule the broadcast REQ packet transmission. For example, the timeline in Fig. 7 shows that the gateway node advances its REQ packet transmission by two data packet slots (D2 and D3). Hereafter this number of data packet slots is denoted by  $N_{\text{adv}}$ . The sooner it is possible to transmit the REQ packet for the next data frame, the better the channel throughput will be. Therefore, we maximize the value for  $N_{\text{adv}}$  under the following constraint:

$$N_{\text{adv}} = \max_{n=1 \dots N} \{ n | n(T_{\text{dp}}[n] + T_{g,[n]}) + T_{\text{rp}} + T_{g,\text{rp}} < 2\tau_p[N+1-n] \}, \quad (7)$$

where  $T_{g,\text{rp}}$  is the guard interval between a REQ packet transmission and the subsequent data packet reception. This constraint ensures that, for every sensor node whose time slot comes later than the REQ packet slot (e.g. nodes 2 and 3 in Fig. 7), it does not arrive at the given node before it has finished transmitting the previous data packet. If this constraint cannot be satisfied for  $n = 1$ , then  $N_{\text{adv}} = 0$ .

### E. ATDA-MAC: CALCULATING TRANSMIT DELAYS

After the gateway node has established the exact time slot for the REQ packet transmission in terms of  $N_{\text{adv}}$ , it can calculate the Tx delays that need to be assigned to every sensor node. We start by calculating a vector of hypothetical

Tx delays  $\tau_{tx}^* = (\tau_{tx}^*[1], \tau_{tx}^*[2], \dots, \tau_{tx}^*[N])$  that would result in a perfect slotted structure, such as that depicted in Fig. 7. The procedure is largely the same as that described for the original TDA-MAC algorithm. We start by assigning the node 1 zero Tx delay,  $\tau_{tx}^*[1] = 0$ . We then iterate through all nodes and assign them Tx delays using the formula given by (1), with the exception of one node, if any, whose data packet slot is scheduled straight after the REQ packet transmission, i.e. if  $n = N - N_{adv} + 1$ . For this node, the following modified formula is used:

$$\begin{aligned}\tau_{tx}^*[n] &= \tau_{tx}^*[n-1] + T_{dp}[n-1] + T_g[n-1] \\ &\quad - 2(\tau_p[n] - \tau_p[n-1]) + T_{rp} + T_{g,RP} \quad (8)\end{aligned}$$

This formula takes into account an extra delay required for inserting a REQ packet transmission before this node's scheduled data packet reception.

Another difference in deriving the Tx delay vector between ATDA-MAC and the original algorithm, is that we do not yet impose constraint (2) on  $\tau_{tx}^*[n]$ , i.e. forcing the transmit delays to be non-negative values, since it could result in channel utilization gaps such as those shown in Fig. 6. We refer to this vector as *hypothetical* Tx delays  $\tau_{tx}^*$ , because some of its values can be negative depending on the node density, in particular on the difference in propagation delays to consecutively scheduled nodes.

If there are any negative values in  $\tau_{tx}^*$ , we introduce a *minimum first node delay* term  $\tau_{min}$ , that ensures that none of the actual assigned Tx delays to the nodes are negative:

$$\tau_{min} = \begin{cases} 0, & \min_n \{\tau_{tx}^*[n]\} \geq 0 \\ -\min_n \{\tau_{tx}^*[n]\}, & \min_n \{\tau_{tx}^*[n]\} < 0 \end{cases} \quad (9)$$

#### F. ATDA-MAC: MINIMUM FRAME LENGTH

We now need to establish the smallest interval at which the gateway node can transmit the broadcast REQ packets, which is also the duration of the TDMA-like frame  $T_{frame}$ , during which the data packets from all sensors are received and a broadcast REQ packet is transmitted. In ATDA-MAC,  $T_{frame}$  is subject to two constraints:

$$\begin{aligned}T_{frame} &\geq T_{min,delay} \\ T_{frame} &\geq T_{min,channel} \quad (10)\end{aligned}$$

where  $T_{min,delay}$  is the constraint due to the propagation delays between the gateway node and the sensor nodes, and  $T_{min,channel}$  is another constraint due to the channel bitrate limit, i.e. if the propagation delays are not the limiting factor, the performance will be limited by the packet duration under full buffer traffic conditions.

The propagation delay constraint  $T_{min,delay}$  is calculated differently in two different cases depicted in Fig. 8:

- the REQ packet is transmitted in a slot between two data packets, or after the final one ( $N_{adv} < N$ , Fig. 8a),
- the REQ packet is transmitted in a slot before all data packets in the current set ( $N_{adv} = N$ , Fig. 8b).

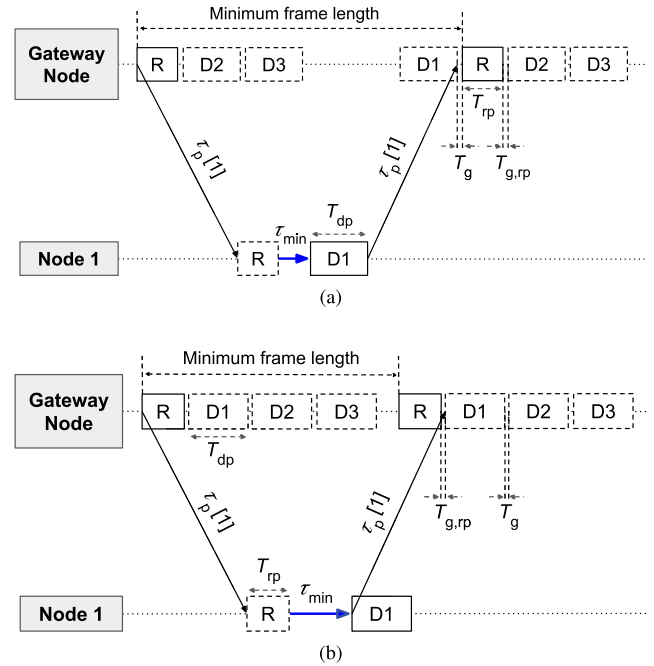


**FIGURE 8. Propagation delay constraint on the minimum frame length in Accelerated TDA-MAC; R - data request (REQ) packet, D - data packet.**  
**(a)** REQ packet is transmitted in a slot between data packets ( $N_{adv} < N$ ).  
**(b)** REQ packet is transmitted before all data packets ( $N_{adv} = N$ ).

In the first case, if  $N_{adv} < N$ ,  $T_{min,delay}$  is calculated using the following expression:

$$\begin{aligned}T_{min,delay} &= 2 \min_n \{\tau_p[n]\} + \tau_{min} + T_{rp} \\ &\quad + \sum_{n=1}^{N-N_{adv}} (T_{dp}[n] + T_g[n]) \quad (11)\end{aligned}$$

It is derived from the timeline depicted in Fig. 8a, which specifies all events, i.e. propagation delays, packet transmissions/receptions and guard intervals, that take place between two consecutive transmissions of the REQ packets.

In the second case, where the REQ packet is transmitted in a slot before all data packets, i.e. if  $N_{adv} = N$ , the expression to calculate  $T_{min,delay}$  derived from the timeline in Fig. 8b is the following:

$$\begin{aligned}T_{min,delay} &= 2 \min_n \{\tau_p[n]\} + T_{rp} + \tau_{min} - T_{g,RP} - T_{rp} \\ &= 2 \min_n \{\tau_p[n]\} + \tau_{min} - T_{g,RP} \quad (12)\end{aligned}$$

The channel bitrate constraint on  $T_{frame}$  is quantified by the following expression:

$$T_{min,channel} = \sum_{n=1}^N (T_{dp}[n] + T_g[n]) + T_{rp} + T_{g,RP} \quad (13)$$

which simply states that  $T_{frame}$  cannot be smaller than the duration of all data packets and one REQ packet, including the guard intervals between them.

Taking both constraints into account, the minimum possible interval between two consecutive REQ packet transmissions can then be expressed as:

$$T_{\text{frame,min}} = \max(T_{\min,\text{delay}}, T_{\min,\text{channel}}) \quad (14)$$

#### G. ATDA-MAC: FINAL ASSIGNMENT OF TRANSMIT DELAYS

Having established the constraints on  $T_{\text{frame}}$ , we can finish calculating the assigned Tx delays to the sensor nodes, by determining the extra delay by which the values in  $\tau_{\text{tx}}^*$  need to be shifted to achieve the ATDA-MAC packet structure, such as that depicted in Fig. 7. Note that  $\tau_{\text{tx}}^*$  is the vector of hypothetical Tx delays that does not take into account any constraints on its values.

Firstly, if  $T_{\text{frame}}$  is constrained by the channel bitrate rather than the propagation delays, i.e. if  $T_{\min,\text{channel}} > T_{\min,\text{delay}}$ , an extra delay term is required to ensure that the gateway node has sufficient time to receive  $N$  data packets between two consecutive REQ packet transmissions. The overall Tx delay shift, which also takes into account the minimum first node delay  $\tau_{\min}$  calculated in (9), is given by:

$$\tau_{\text{shift}} = \tau_{\min} + \begin{cases} 0, & \Delta T_{\min} \geq 0 \\ -\Delta T_{\min}, & \Delta T_{\min} < 0, \end{cases} \quad (15)$$

where:

$$\Delta T_{\min} = T_{\min,\text{delay}} - T_{\min,\text{channel}} \quad (16)$$

Finally, the values for the assigned Tx delays to every sensor node  $\tau_{\text{tx}}$  can be calculated by shifting the originally calculated hypothetical values in  $\tau_{\text{tx}}^*$  as follows:

$$\forall n \in [1, N], \quad \tau_{\text{tx}}[n] = \tau_{\text{tx}}^*[n] + \tau_{\text{shift}} + (T_{\text{frame}} - T_{\text{frame,min}}) \quad (17)$$

There, an extra term  $T_{\text{frame}} - T_{\text{frame,min}}$  is included for the cases where the desired frequency of data frames is below the system capacity. For example, if the sensor readings are collected less frequently than  $1/T_{\text{frame,min}}$ . However, if the MAC layer is required to operate at maximum capacity and minimum latency,  $T_{\text{frame}}$  should be set to  $T_{\text{frame,min}}$ , therefore  $T_{\text{frame}} - T_{\text{frame,min}}$  will be zero.

#### H. CHANNEL UTILIZATION OF ATDA-MAC

Similarly to Equation (4) for TDA-MAC, the following expression describes the maximum channel utilization achievable with ATDA-MAC:

$$\gamma_{\max} = \frac{\sum_{n=1}^N T_{\text{dp}}[n]}{\sum_{n=1}^N (T_{\text{dp}}[n] + T_g[n]) + T_{\text{rp}} + T_{g,\text{rp}}} \quad (18)$$

It states that the loss of throughput only occurs due to the guard intervals and the time it takes to transmit the REQ packet in a time slot between the data packets. Unlike the TDA-MAC algorithm proposed in Subsection III-A, the

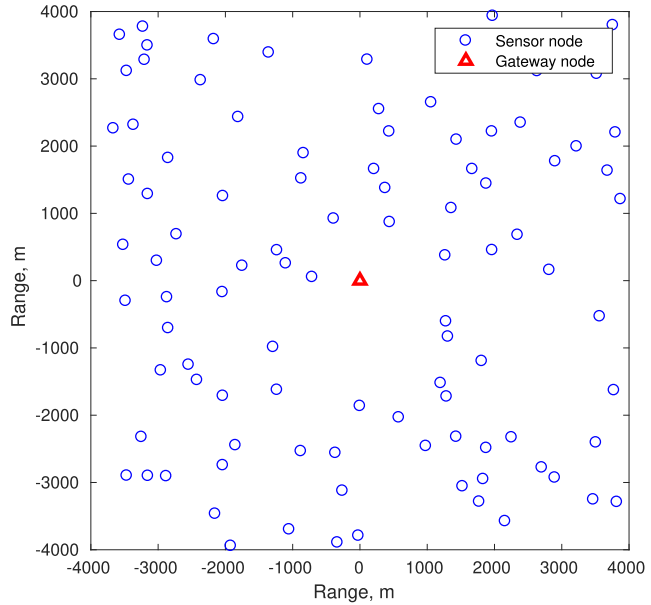


**FIGURE 9.** Top view of the simulated network topology; depth of gateway node - 5 m, depth of sensor nodes - random between 480-500 m.

channel utilization is no longer limited by the distribution of the propagation delays, which allows it to achieve higher throughputs in scenarios with shorter packet lengths and fewer nodes.

## IV. SIMULATION RESULTS

In this section we evaluate the performance of TDA-MAC and ATDA-MAC using a MATLAB simulation model of the oil reservoir seismic monitoring network depicted in Fig. 1b. We compare the performance of the two proposed schemes with that of an optimal synchronized staggered TDMA approach [5], sequential polling and T-Lohi [12] under periodic data gathering and random Poisson traffic conditions [26].

#### A. SIMULATION SETUP

The simulated network topology is shown in Fig. 9. Sensor nodes are randomly distributed across an 8×8 km coverage area using Matérn Hard-core Point Process [34] with the minimum horizontal distance between the nodes of 200 m. The depth of sensor nodes follows a uniform random distribution between 480 and 500 m. These parameters correspond to a typical oil reservoir seismic monitoring scenario, e.g. [23]. The gateway node is positioned above the center of the coverage area at 5 m depth.

The propagation delays between every pair of nodes were measured using the BELLHOP ray tracing program [20], a well-established platform for simulating underwater acoustic wave propagation. In order to avoid a significant increase in simulation time due to BELLHOP ray tracing, we have employed a grid approach similar to that used in the VirTEX simulator [35]. First, we ran BELLHOP simulations with a fine 1m grid of source/receiver ranges and depths across the

full range of the simulated coverage area, i.e.  $8 \times 8$  km at 5 m and 480-500 m depths. The results of this simulation are saved in a data file used as a look-up table for the propagation delay values of the strongest echoes, i.e. typically the direct/shortest propagation paths. Afterwards, all randomly generated node positions were moved to the nearest 1m grid points in order to use the exact outputs previously produced by the BELLHOP simulation.

**TABLE 2.** Simulation scenarios.

|          | Number of nodes | Channel bitrate | Packet length | Packet duration |
|----------|-----------------|-----------------|---------------|-----------------|
| <b>1</b> | 100             | 100 b/s         | 512 bits      | 5.12 sec        |
| <b>2</b> | 100             | 100 b/s         | 64 bits       | 0.64 sec        |
| <b>3</b> | 50              | 1400 b/s        | 256 bits      | 0.183 sec       |
| <b>4</b> | 20              | 9200 b/s        | 4096 bits     | 0.445 sec       |

Table 2 summarizes four different scenarios used in our simulations in terms of the number of nodes and packet lengths. The first two scenarios assume large networks of low-cost spread spectrum acoustic modems operating at 100 b/s, such as those developed at the University of Newcastle [33]. Scenario 1 evaluates the network performance with long packets (512 bits), relative to the propagation delays, whereas Scenario 2 uses much shorter packets (64 bits). Scenario 3 corresponds to a smaller network (50 nodes) of higher data rate acoustic modems (1400 b/s), also discussed in [33], with relatively short packet lengths. Finally, Scenario 4 represents an even smaller network of high cost, high data rate modems, e.g. EvoLogics S2CR 15/27 [36]. These four scenarios provide a range of different test cases for evaluating the performance of our proposed MAC schemes, compared with the existing approaches in the literature.

The length of control packets used in the four scenarios is 32, 32, 64 and 1024 bits respectively, i.e. a quarter of the data packet length or at least 32 bits, which corresponds to realistic control packet lengths for the different modems considered. To ensure statistically valid conclusions, all simulation results presented in this section are based on 50 simulations with different random node locations, each simulation lasting 10,000 data packet transmissions. All data points in the plots are derived from the mean of 50 simulations, while the error bars represent the 5th and 95th percentiles. For the data points where the error bars are not visible, the variation between the 5th and 95th percentile is negligible.

## B. PERIODIC DATA GATHERING SIMULATIONS

Fig. 10 shows the periodic data gathering network throughput when the gateway node collects data from all sensor nodes as frequently as possible. Here, throughput is defined as physical layer throughput, i.e. how many bits per second is received at the gateway node including all header and footer data. In addition to TDA-MAC and ATDA-MAC, the graphs include the performance of ideal synchronized TDMA and

sequential polling for baseline comparison. In the synchronized TDMA approach, every sensor node is scheduled to transmit their packets in particular time slots, such that all packets arrive in a TDMA frame at the gateway node [5]. In the sequential polling approach, the gateway node transmits a short data request packet to an individual sensor node and then waits for its data packet, before doing the same with the next node and so on. The plots in Fig. 10 also compare the simulated performance of TDA-MAC and ATDA-MAC with best case analytical predictions of proportional network throughput, given by Equations (4) and (18), multiplied by the channel capacity.

Firstly, there is negligible difference in throughput performance between ATDA-MAC and synchronized staggered TDMA in all four simulated scenarios. This demonstrates that ATDA-MAC can achieve the performance of ideal synchronized TDMA in the periodic data gathering scenario without the need for clock synchronization among the sensor nodes. For both proposed algorithms, the dominant source of throughput loss is the use of a TDMA guard interval between data packets, which is assumed to be 5% of the data packet duration. In more realistic deployments, the duration of the guard interval can be adjusted to allow for the multipath spread and for inaccuracies in estimating the propagation delays.

Secondly, the performance of the TDA-MAC protocol matches the performance of ATDA-MAC and synchronized TDMA in the first two scenarios. This is because with large numbers of nodes (in this case 100) and sufficiently long packets, the propagation delay distribution plays a negligible role compared with the time it takes to receive all 100 data packets. In contrast, in Scenarios 3 and 4 which involve fewer nodes and/or shorter packets, TDA-MAC suffers from some throughput loss, compared with synchronized TDMA and ATDA-MAC. However, in all cases our proposed algorithms significantly outperform a straightforward sequential polling approach, which works most efficiently with longer packets, because the channel is reserved for one node transmission at a time.

Furthermore, the comparison between simulations of the proposed MAC protocols and the analytical predictions of their network throughput in Fig. 10 shows that Equations (4) and (18) provide a good estimate of system performance based on the network deployment parameters, e.g. packet duration and the minimum propagation delay. The slight discrepancy between the analytically predicted best case performance of TDA-MAC and the simulation outcome in Scenarios 3 and 4 is due to the combination of node sparsity and short packet duration with respect to the propagation delays, which sometimes causes channel utilization gaps between data packet slots, such as those illustrated in Fig. 6.

Table 3 summarizes the periodic data gathering interval achieved by the four MAC protocols in the four different scenarios. For example, in Scenario 1 with a large number of low-cost 100 b/s nodes and long packets (5.12 s duration), a full set of data packets from all nodes can be collected

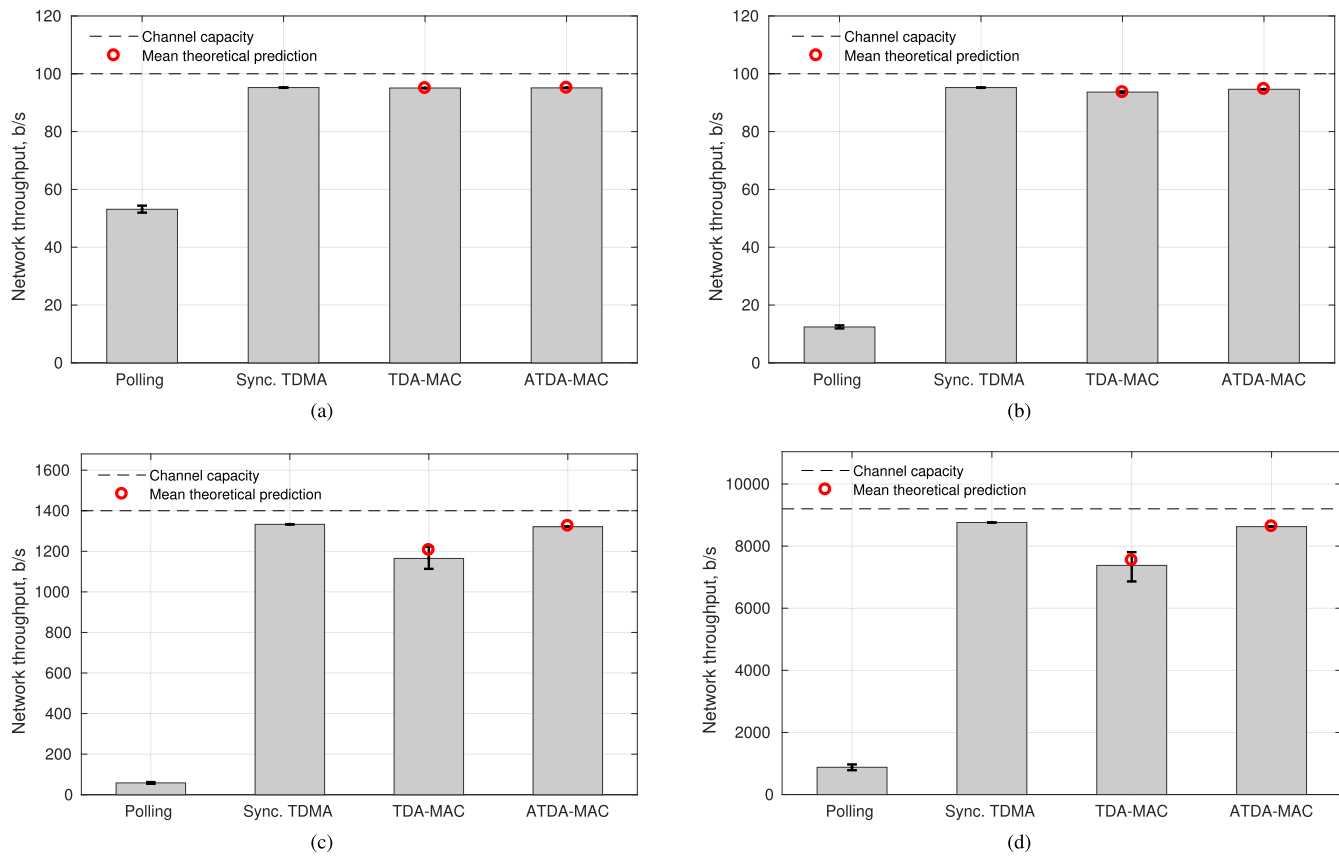


**FIGURE 10.** Network throughput achieved by sequential polling, synchronized staggered TDMA, TDA-MAC and ATDA-MAC under periodic data collection traffic conditions. The simulation results of TDA-MAC and ATDA-MAC are compared with analytical predictions using Equations (4) and (18). (a) Scenario 1: 100 nodes, 100 b/s channel, 512 bit packet length. (b) Scenario 2: 100 nodes, 100 b/s channel, 64 bit packet length. (c) Scenario 3: 50 nodes, 1.4 kb/s channel, 256 bit packet length. (d) Scenario 4: 20 nodes, 9.2 kb/s channel, 4096 bit packet length.

**TABLE 3.** Fastest achievable data gathering period using sequential polling, synchronized staggered TDMA, TDA-MAC and ATDA-MAC (mean  $\pm$  standard deviation).

|                                             | Polling                 | Sync. TDMA            | TDA-MAC                 | ATDA-MAC              |
|---------------------------------------------|-------------------------|-----------------------|-------------------------|-----------------------|
| <b>100 nodes, 100 b/s, 512 bit packets</b>  | $964 \pm 13\text{ s}$   | $538 \pm 0\text{ s}$  | $538 \pm 0\text{ s}$    | $538 \pm 0\text{ s}$  |
| <b>100 nodes, 100 b/s, 64 bit packets</b>   | $516 \pm 13\text{ s}$   | $67.2 \pm 0\text{ s}$ | $68.3 \pm 0.1\text{ s}$ | $67.6 \pm 0\text{ s}$ |
| <b>50 nodes, 1.4 kb/s, 256 bit packets</b>  | $219 \pm 10\text{ s}$   | $9.60 \pm 0\text{ s}$ | $11.0 \pm 0.3\text{ s}$ | $9.69 \pm 0\text{ s}$ |
| <b>20 nodes, 9.2 kb/s, 4096 bit packets</b> | $93.6 \pm 6.2\text{ s}$ | $9.35 \pm 0\text{ s}$ | $11.1 \pm 0.4\text{ s}$ | $9.50 \pm 0\text{ s}$ |

approximately every 16 minutes via sequential polling, whereas the TDA-MAC protocol can do it every 9 minutes. If the packet length is reduced to 64b (Scenario 2), sequential polling takes 8.6 minutes, whereas TDA-MAC and ATDA-MAC provide a dramatic improvement and are capable of collecting data almost every minute if necessary. The performance difference is even more significant in Scenarios 3 and 4, with fewer nodes and/or shorter packets. Furthermore, similarly to the bar plots in Fig. 10, Table 3 shows that the performance of ATDA-MAC closely matches the performance of the ideal synchronized TDMA approach, but without assuming clock synchronization among sensor nodes. The slight difference in the maximum data gathering

interval achieved by the two schemes is due to the duration of the REQ packet transmission in ATDA-MAC, which is not present in the synchronized TDMA approach. The small variability in the data gathering period shown in Table 3 for sequential polling and TDA-MAC stems from the propagation delays of randomly positioned sensor nodes in 50 different simulations. The frame duration of TDA-MAC depends on the propagation delay distribution from the gateway node to the sensor nodes. Similarly, the performance of sequential polling depends on the mean propagation delay, i.e. how long it takes for sensor nodes to receive a data request and transmit data back to the gateway node. In contrast, the throughput performance of synchronized TDMA and ATDA-MAC does

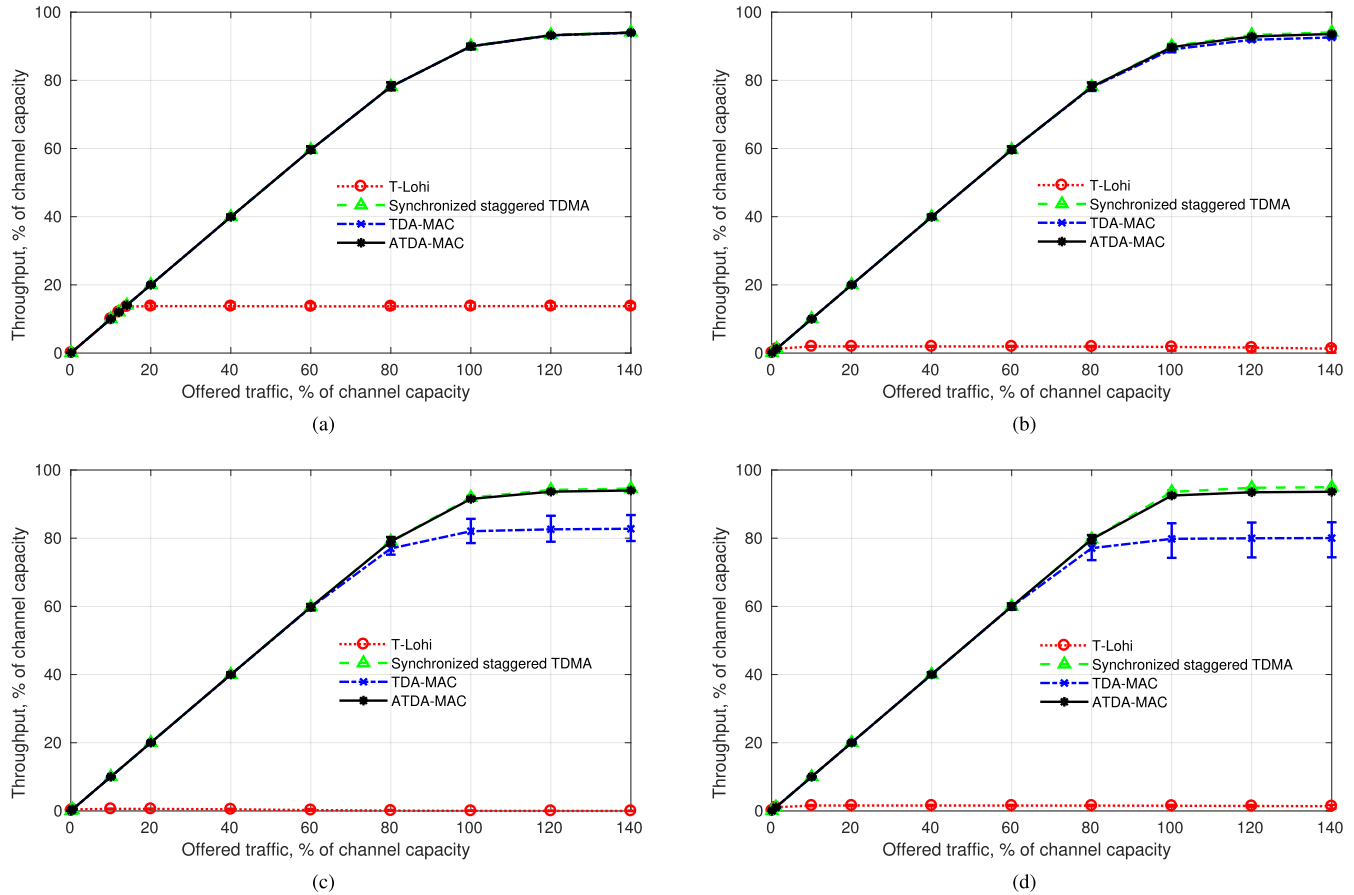


**FIGURE 11.** Network throughput achieved by T-Lohi, synchronized staggered TDMA, TDA-MAC and ATDA-MAC under Poisson traffic conditions.

(a) Scenario 1: 100 nodes, 100 b/s channel, 512 bit packet length. (b) Scenario 2: 100 nodes, 100 b/s channel, 64 bit packet length.  
 (c) Scenario 3: 50 nodes, 1.4 kb/s channel, 256 bit packet length. (d) Scenario 4: 20 nodes, 9.2 kb/s channel, 4096 bit packet length.

not depend on the propagation delays, since the transmissions are scheduled in a way that ensures an uninterrupted flow of packets.

### C. RANDOM POISSON TRAFFIC SIMULATIONS

In this subsection we present the results of simulations based on Poisson traffic, i.e. random exponentially distributed packet inter-arrival times at every sensor node. Although it is irrelevant for some wireless sensor network deployment scenarios, e.g. periodic data gathering for environmental monitoring applications, it is a classical traffic model used to compare MAC schemes, e.g. [12], [13], and would be representative of applications characterized by naturally occurring events with no correlation among different nodes. In these simulations we compare the performance of our proposed algorithms with the synchronized staggered TDMA approach (same as in the last subsection) and T-Lohi [12], a classical contention-based MAC scheme designed for underwater acoustic networks with sporadic traffic, and commonly used for baseline comparison. Here we use a synchronized version of T-Lohi, i.e. where contention rounds start synchronously at all nodes. For fair comparison, the duration of the contention tone is 50 ms, i.e. significantly smaller than the control packet duration in TDA-MAC and ATDA-MAC.

Fig. 11 shows the network throughput at different traffic loads, where both are expressed as percentage of the overall channel capacity (i.e. bitrate). Firstly, the plots show that the maximum throughput achieved by TDA-MAC and ATDA-MAC is consistent with that shown in Fig. 10 for periodic data gathering traffic. The throughput at lower and medium traffic loads linearly increases with the traffic load, which demonstrates that the proposed protocols work well as generalized TDMA-based MAC schemes, not only for periodic data gathering. Secondly, it shows that TDA-MAC and ATDA-MAC achieve significantly higher network throughput than the contention based T-Lohi protocol, because the latter is severely limited by the propagation delays with respect to the packet duration. T-Lohi performs better in the long packet scenario (Scenario 1), because the time it takes to reserve the channel is comparable with the duration of the subsequent packet transmission. However, the scheduled TDA-MAC and ATDA-MAC protocols are far better suited to the other three scenarios, where the packet duration is smaller than most propagation delays in the network.

Another important performance metric that is relevant under random bursty traffic conditions is the end-to-end packet delay, i.e. how long it takes for a data packet to be received at the gateway node from the moment it is created

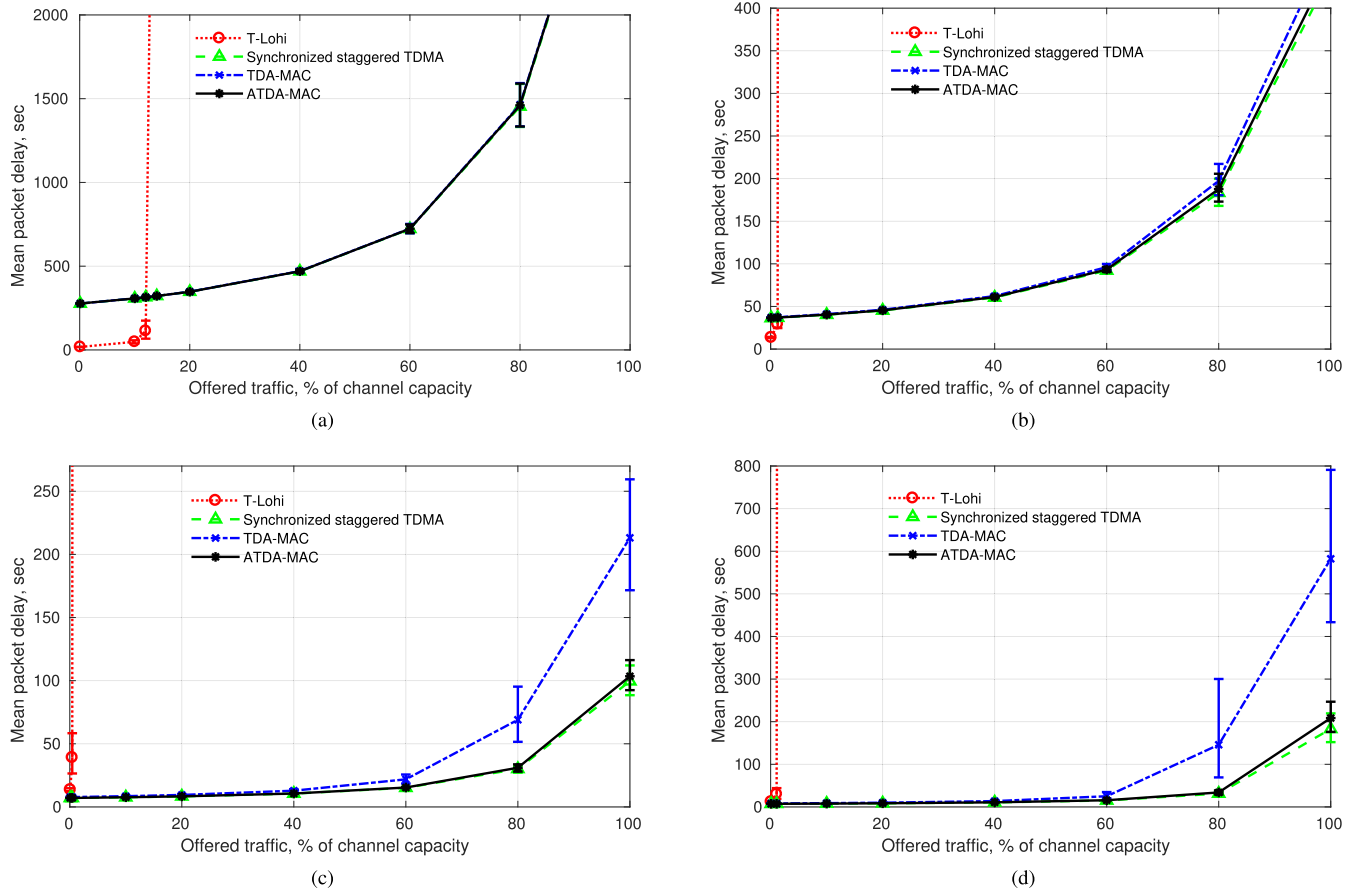


**FIGURE 12.** Mean end-to-end packet delays achieved by T-Lohi, synchronized staggered TDMA, TDA-MAC and ATDA-MAC. (a) Scenario 1: 100 nodes, 100 b/s channel, 512 bit packet length. (b) Scenario 2: 100 nodes, 100 b/s channel, 64 bit packet length. (c) Scenario 3: 50 nodes, 1.4 kb/s channel, 256 bit packet length. (d) Scenario 4: 20 nodes, 9.2 kb/s channel, 4096 bit packet length.

at the application layer and passed down to the MAC layer for transmission. Fig. 12 shows the mean packet delay at the full range of traffic loads using four different MAC schemes. Firstly, there is negligible difference between the mean packet delay achieved by ATDA-MAC and synchronized TDMA. Furthermore, in Scenarios 1 and 2, both involving 100 nodes and sufficiently long packets, TDA-MAC also roughly matches the performance of synchronized TDMA. In Scenarios 3 and 4, the packet delays achieved by ATDA-MAC at high traffic loads are smaller than those achieved by TDA-MAC due to the higher maximum throughput of the former, as shown in Fig. 11c and 11d. In general, the packet delays start to increase exponentially once the offered traffic exceeds the maximum network throughput of a given MAC scheme. Severe network throughput limits are the reason why the packet delays achieved by T-Lohi increase rapidly with traffic load. Nevertheless, Fig. 12a shows that TDA-MAC and ATDA-MAC can be less efficient in terms of packet delay at low traffic loads than contention based algorithms such as T-Lohi. This is because, in T-Lohi, several nodes are unlikely to contend for the channel at the same time at low traffic loads, so the time it takes for a node to reserve the channel is small. In contrast, in scheduled TDMA-based schemes the nodes

always have to wait for their assigned timing slot to transmit the data packet. The relative performance of T-Lohi and the TDMA-based schemes at low traffic loads in Scenarios 2-4 is difficult to judge from the plots in Fig. 12, and, therefore, is examined in more detail in Subsection IV-D.

Fig. 13 shows the cumulative distribution function (CDF) of the end-to-end packet delay at 80% traffic load. The plots show that the packet delay performance of ATDA-MAC follows the same distribution as the ideal synchronized TDMA approach in all four simulated scenarios. In Scenarios 3 and 4, the packet delays achieved by TDA-MAC are longer across the whole distribution, not just the mean or high percentile (tail) performance. This is due to the difference in TDMA frame length, constrained by the propagation delay distribution in TDA-MAC, as discussed in Subsection III-B. This results in longer waiting times for the nodes to transmit their packets when two or more packets are queued up and a node has to wait an entire TDMA frame between any two transmissions.

#### D. PERFORMANCE AT LOW TRAFFIC LOADS

Fig. 14 shows the same type of mean packet delay plots as Fig. 12, but zooms in on the low traffic region in all four

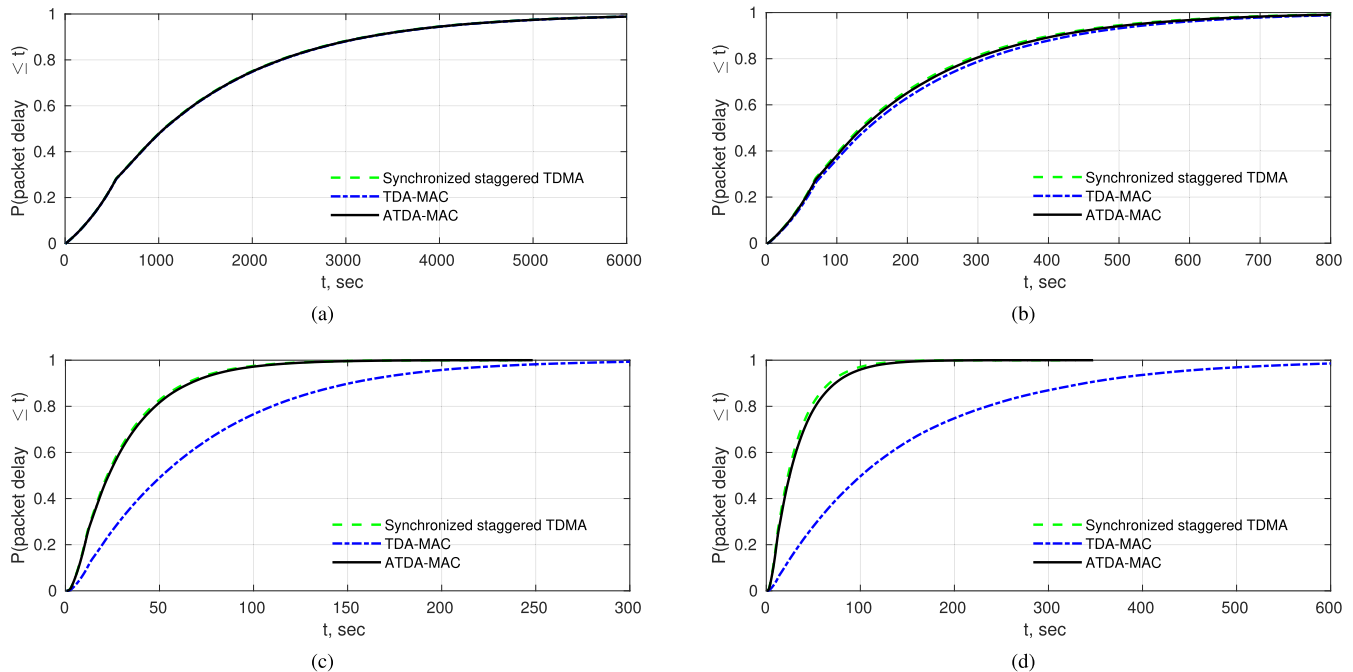


**FIGURE 13.** Distribution of the end-to-end packet delay achieved by synchronized staggered TDMA, TDA-MAC and ATDA-MAC at 80% traffic load.  
**(a)** Scenario 1: 100 nodes, 100 b/s channel, 512 bit packet length. **(b)** Scenario 2: 100 nodes, 100 b/s channel, 64 bit packet length.  
**(c)** Scenario 3: 50 nodes, 1.4 kb/s channel, 256 bit packet length. **(d)** Scenario 4: 20 nodes, 9.2 kb/s channel, 4096 bit packet length.

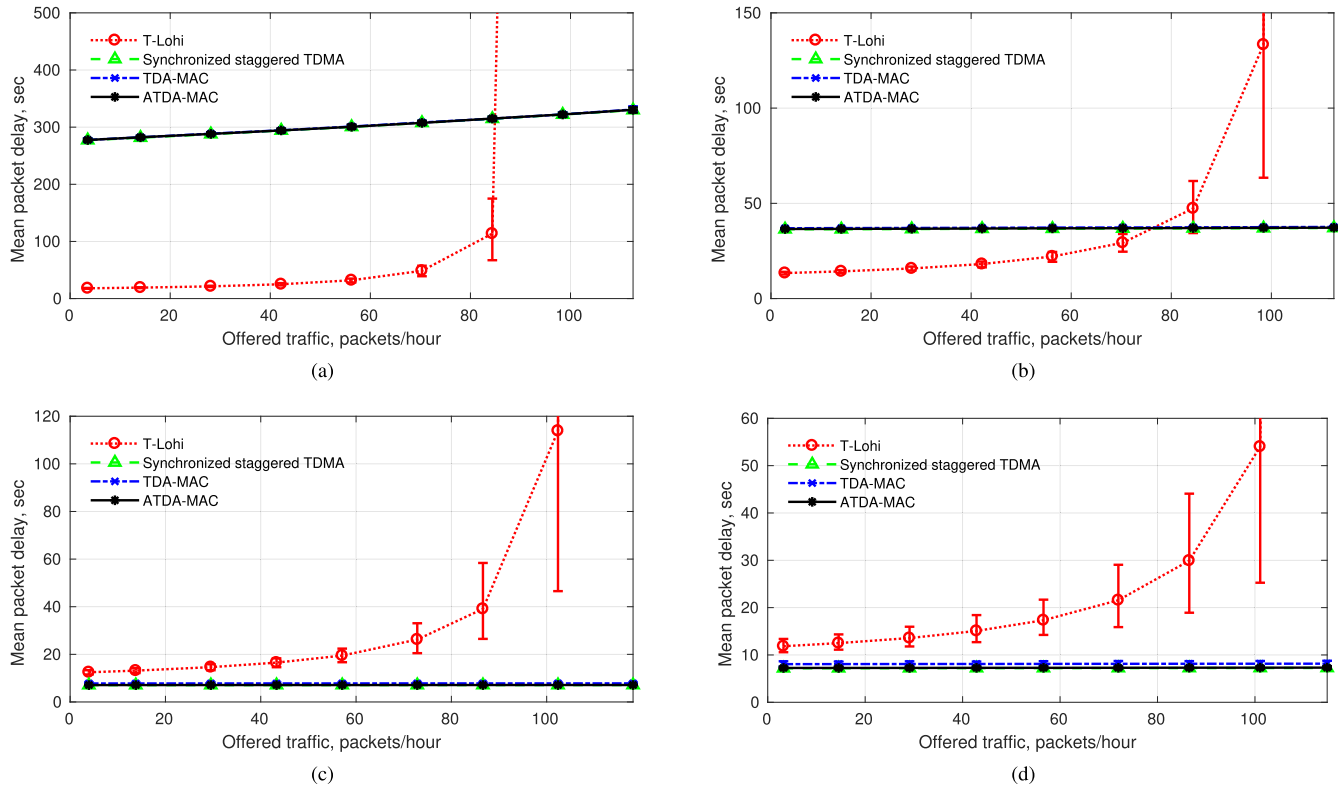


**FIGURE 14.** Mean end-to-end packet delays achieved by T-Lohi, synchronized staggered TDMA, TDA-MAC and ATDA-MAC at low traffic loads. **(a)** Scenario 1: 100 nodes, 100 b/s channel, 512 bit packet length. **(b)** Scenario 2: 100 nodes, 100 b/s channel, 64 bit packet length. **(c)** Scenario 3: 50 nodes, 1.4 kb/s channel, 256 bit packet length. **(d)** Scenario 4: 20 nodes, 9.2 kb/s channel, 4096 bit packet length.

scenarios. In these plots, the offered traffic load is expressed in packets/hour, as opposed to the proportion of the channel bitrate, because T-Lohi is predominantly constrained by the

propagation delays which are the same across all four simulated scenarios. For example, a traffic load of 100 packets/hour translates into approximately 14% of channel capacity

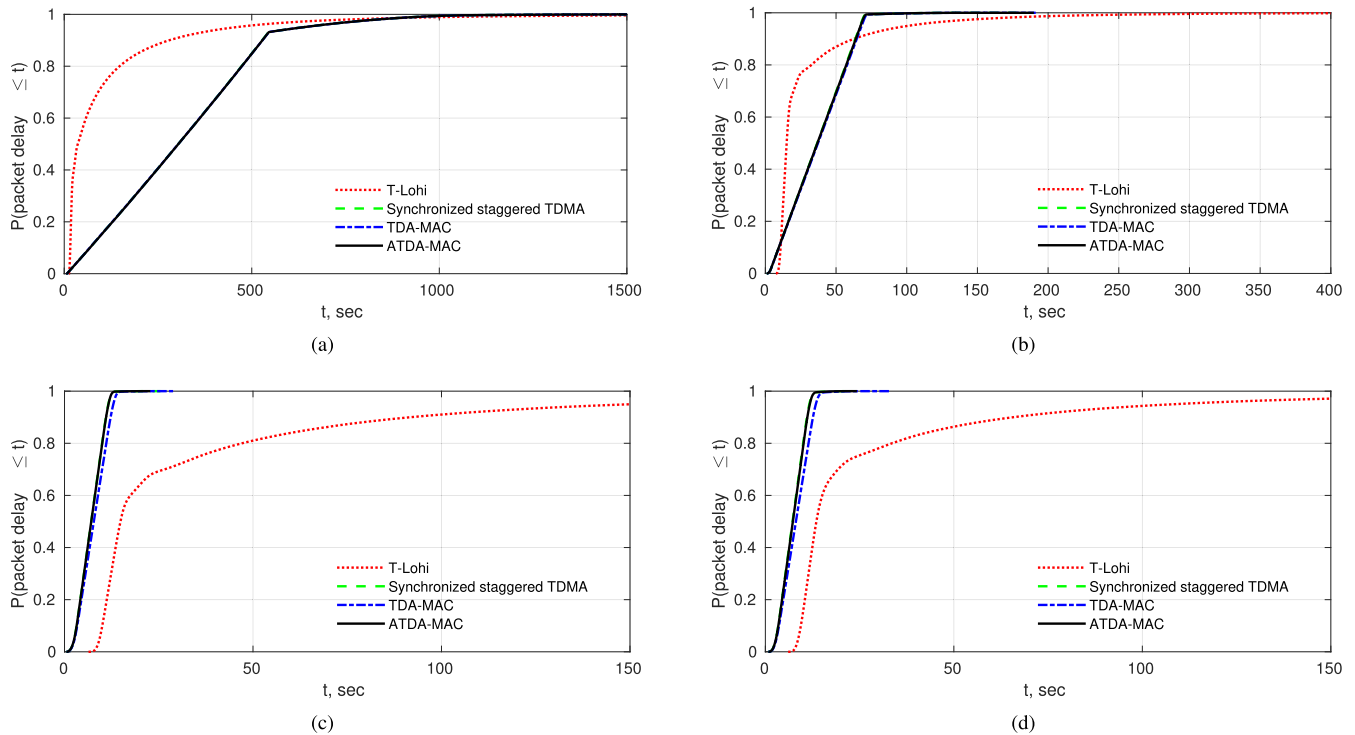


**FIGURE 15.** End-to-end packet delay achieved by T-Lohi, synchronized staggered TDMA, TDA-MAC and ATDA-MAC at  $\approx 90$  packets/hour offered traffic. (a) Scenario 1: 100 nodes, 100 b/s channel, 512 bit packet length. (b) Scenario 2: 100 nodes, 100 b/s channel, 64 bit packet length. (c) Scenario 3: 50 nodes, 1.4 kb/s channel, 256 bit packet length. (d) Scenario 4: 20 nodes, 9.2 kb/s channel, 4096 bit packet length.

in Scenario 1 and only 0.5% of channel capacity in Scenario 3 due to the difference in packet length and channel bitrate.

Fig. 14a shows that in a scenario with a large number of nodes and long packet duration, the proposed protocols are inefficient at very low traffic loads due to excessively long TDMA frame lengths. Here, the mean packet delay of TDA-MAC and ATDA-MAC is roughly an order of magnitude longer compared with the contention-based T-Lohi approach. Fig. 14b shows that, if the packet duration is reduced, the packet delay performance of TDA-MAC and ATDA-MAC is significantly improved, because the decrease in packet size causes a proportional decrease in the TDMA frame duration. However, the mean packet delay with such a high number of nodes is still longer than that of T-Lohi. In contrast, in Scenarios 3 and 4 with fewer nodes and shorter packets, the packet delay performance of the proposed protocols is better than the T-Lohi performance even at very low traffic loads. This is because, in these scenarios, the TDMA frame length, i.e. the interval between two consecutive opportunities for any sensor node to transmit data, is comparable to the maximum propagation delay between sensor nodes, which dictates the duration of a contention round in T-Lohi. This means that the typical waiting time until a node's next opportunity to transmit in a TDMA setting is smaller than the time it takes for a node to win contention for a channel in T-Lohi.

Fig. 15 shows the CDFs of the end-to-end delays of all simulated packets at a traffic load of approximately 90 packets/hour. Firstly, because this is a far lower traffic load

compared to that used in Fig. 13, the long-tail feature of the packet delay distribution has largely disappeared for TDMA-based MAC schemes. This is because it is highly unlikely for any node to have more than one packet in its queue at such a low traffic load. There, the packet delay performance is only affected by the propagation delays and the timing of random packet arrivals with respect to the timing of a given node's TDMA slot. In contrast, the packet delay distribution of T-Lohi has a pronounced long-tail, because even at 90 packets/hour offered traffic it is operating close to its maximum throughput, which means that many packet transmissions get backed off or queued up until future contention opportunities.

## V. CONCLUSION

In this paper, we have proposed two MAC protocols for underwater acoustic sensor networks, namely Transmit Delay Allocation MAC (TDA-MAC) and Accelerated TDA-MAC (ATDA-MAC), that are capable of providing TDMA-based channel access to the network nodes without the need for centralized clock synchronization.

A comprehensive simulation study of a UAN deployed on the sea bed showed that the proposed protocols were able to closely match the throughput and packet delay performance of the ideal synchronized TDMA approach in single-hop underwater acoustic networks. In particular, the efficient pattern of broadcast control packet transmissions and received data packets allowed ATDA-MAC to perform as well as the ideal TDMA approach in all simulated scenarios,

ranging from a network of 20 high-cost high data rate acoustic modems to a network of 100 low-cost modems operating at a data rate of 100 bits per second. The proposed protocols achieve far higher throughput than T-Lohi, a classical contention-based MAC protocol designed for UANs. In scenarios with short packet lengths and fewer than 50 nodes, TDA-MAC and ATDA-MAC produce better end-to-end packet delay performance even at low traffic loads compared with T-Lohi, although traditionally this has been a drawback of TDMA-based MAC protocols compared with contention-based schemes. This is because large propagation delays have little effect on the time interval at which the nodes can transmit packets in TDA-MAC and ATDA-MAC, whereas the T-Lohi channel reservation process is severely slowed down because of them.

Furthermore, the MAC functionality required to be implemented on the sensor nodes is minimal; they wait for a particular type of control packet and transmit one predefined control/data packet in response. All complexity of controlling the operation of the network is at the gateway node base station. Crucially, there is also no need for clock synchronization across the sensor nodes, which is a major advantage of TDA-MAC and ATDA-MAC compared with other scheduled TDMA protocols in the literature. These features make the proposed protocols a feasible networking solution for real-world cost-efficient UAN deployments.

## REFERENCES

- [1] G. Acar and A. E. Adams, "ACMENet: An underwater acoustic sensor network protocol for real-time environmental monitoring in coastal areas," *IEE Proc.-Radar, Sonar Navigat.*, vol. 153, no. 4, pp. 365–380, Aug. 2006.
- [2] J. Heidemann, M. Stojanovic, and M. Zorzi, "Underwater sensor networks: Applications, advances and challenges," *Philos. Trans. Roy. Soc. London A, Math. Phys. Sci.*, vol. 370, no. 1958, pp. 158–175, Jan. 2012.
- [3] L. Liu, S. Zhou, and J.-H. Cui, "Prospects and problems of wireless communication for underwater sensor networks," *Wireless Commun. Mobile Comput.*, vol. 8, no. 8, pp. 977–994, 2008.
- [4] J. Yackoski and C.-C. Shen, "UW-FLASHR: Achieving high channel utilization in a time-based acoustic mac protocol," in *Proc. 3rd ACM Int. Workshop Underwater Netw. (WuWNet)*, 2008, pp. 59–66.
- [5] K. Kredo, II, P. Djukic, and P. Mohapatra, "STUMP: Exploiting position diversity in the staggered TDMA underwater MAC protocol," in *Proc. IEEE INFOCOM*, Apr. 2009, pp. 2961–2965.
- [6] S. Lmai, M. Chitre, C. Laot, and S. Houcke, "Throughput-efficient super-TDMA MAC transmission schedules in ad hoc linear underwater acoustic networks," *IEEE J. Ocean. Eng.*, vol. 42, no. 1, pp. 156–174, Jan. 2017.
- [7] E. M. Sozer, M. Stojanovic, and J. G. Proakis, "Underwater acoustic networks," *IEEE J. Ocean. Eng.*, vol. 25, no. 1, pp. 72–83, Jan. 2000.
- [8] D. Pompili, T. Melodia, and I. F. Akyildiz, "A CDMA-based medium access control for underwater acoustic sensor networks," *IEEE Trans. Wireless Commun.*, vol. 8, no. 4, pp. 1899–1909, Apr. 2009.
- [9] I. F. Akyildiz, D. Pompili, and T. Melodia, "Underwater acoustic sensor networks: Research challenges," *Ad Hoc Netw.*, vol. 3, no. 3, pp. 257–279, Mar. 2005.
- [10] M. Molins and M. Stojanovic, "Slotted FAMA: A MAC protocol for underwater acoustic networks," in *Proc. IEEE OCEANS*, May 2006, pp. 1–7.
- [11] Y. Noh et al., "DOTS: A propagation delay-aware opportunistic MAC protocol for mobile underwater networks," *IEEE Trans. Mobile Comput.*, vol. 13, no. 4, pp. 766–782, Apr. 2014.
- [12] A. A. Syed, W. Ye, and J. Heidemann, "Comparison and evaluation of the T-Lohi MAC for underwater acoustic sensor networks," *IEEE J. Sel. Areas Commun.*, vol. 26, no. 9, pp. 1731–1743, Dec. 2008.
- [13] W.-H. Liao and C.-C. Huang, "SF-MAC: A spatially fair MAC protocol for underwater acoustic sensor networks," *IEEE Sensors J.*, vol. 12, no. 6, pp. 1686–1694, Jun. 2012.
- [14] C. L. Fullmer and J. J. Garcia-Luna-Aceves, "Floor acquisition multiple access (FAMA) for packet-radio networks," in *Proc. Conf. Appl. Technol., Archit., Protocols Comput. Commun. (SIGCOMM)*, 1995, pp. 262–273.
- [15] N. Chirdchoo, W.-S. Soh, and K. C. Chua, "MU-Sync: A time synchronization protocol for underwater mobile networks," in *Proc. 3rd ACM Int. Workshop Underwater Netw. (WuWNet)*, 2008, pp. 35–42.
- [16] S. Knappe et al., "A microfabricated atomic clock," *Appl. Phys. Lett.*, vol. 85, no. 9, pp. 1460–1462, 2004.
- [17] A. T. Gardner and J. A. Collins, "Advancements in high-performance timing for long term underwater experiments: A comparison of chip scale atomic clocks to traditional microprocessor-compensated crystal oscillators," in *Proc. IEEE OCEANS*, Oct. 2012, pp. 1–8.
- [18] K. G. Kekkal et al., "Underwater acoustic modems with integrated atomic clocks for one-way travel-time underwater vehicle positioning," in *Proc. Underwater Acoust. Conf. Exhib. (UACE)*, 2017, pp. 1–10.
- [19] S. Lmai, M. Chitre, C. Laot, and S. Houcke, "Throughput-maximizing transmission schedules for underwater acoustic multihop grid networks," *IEEE J. Ocean. Eng.*, vol. 40, no. 2, pp. 853–863, Oct. 2015.
- [20] M. Porter. (Sep. 2017). *Acoustics Toolbox*. [Online]. Available: <http://oalib.hisresearch.com/Modes/AcousticsToolbox/>
- [21] A. Khan and L. Jenkins, "Undersea wireless sensor network for ocean pollution prevention," in *Proc. 3rd Int. Conf. Commun. Syst. Softw. Middleware Workshops (COMSWARE)*, 2008, pp. 2–8.
- [22] B. J. Boom et al., "A research tool for long-term and continuous analysis of fish assemblage in coral-reefs using underwater camera footage," *Ecol. Inform.*, vol. 23, pp. 83–97, Sep. 2014.
- [23] A. K. Mohapatra, N. Gautam, and R. L. Gibson, "Combined routing and node replacement in energy-efficient underwater sensor networks for seismic monitoring," *IEEE J. Ocean. Eng.*, vol. 38, no. 1, pp. 80–90, Jan. 2013.
- [24] I. Vasilescu, K. Kotay, D. Rus, M. Dunbabin, and P. Corke, "Data collection, storage, and retrieval with an underwater sensor network," in *Proc. 3rd Int. Conf. Embedded Netw. Sensor Syst.*, 2005, pp. 154–165.
- [25] R. H. Seymour and F. Barr, "An improved seabed seismic 4D data collection method for reservoir monitoring," in *Proc. Eur. Petroleum Conf.*, 1996, pp. 189–194.
- [26] V. S. Frost and B. Melamed, "Traffic modeling for telecommunications networks," *IEEE Commun. Mag.*, vol. 32, no. 3, pp. 70–81, Mar. 1994.
- [27] V. Paxson and S. Floyd, "Wide area traffic: The failure of Poisson modeling," *IEEE/ACM Trans. Netw.*, vol. 3, no. 3, pp. 226–244, Jun. 1995.
- [28] W. E. Leland, M. S. Taqqu, W. Willinger, and D. V. Wilson, "On the self-similar nature of Ethernet traffic (extended version)," *IEEE/ACM Trans. Netw.*, vol. 2, no. 1, pp. 1–15, Feb. 1994.
- [29] C. Li, Y. Xu, C. Xu, Z. An, B. Diao, and X. Li, "DTMAC: A delay tolerant MAC protocol for underwater wireless sensor networks," *IEEE Sensors J.*, vol. 16, no. 11, pp. 4137–4146, Jun. 2016.
- [30] A. Mainwaring, D. Culler, J. Polastre, R. Szewczyk, and J. Anderson, "Wireless sensor networks for habitat monitoring," in *Proc. 1st ACM Int. Workshop Wireless Sensor Netw. Appl.*, 2002, pp. 88–97.
- [31] W. D. Wilson, "Speed of sound in sea water as a function of temperature, pressure, and salinity," *J. Acoust. Soc. Amer.*, vol. 32, no. 6, pp. 641–644, 1960.
- [32] B. Dushaw. (2009). *Worldwide Sound Speed, Temperature, Salinity, and Buoyancy from the NOAA World Ocean Atlas*. [Online]. Available: <http://staff.washington.edu/dushaw/WOA/>
- [33] J. A. Neasham, G. Goodfellow, and R. Sharphouse, "Development of the 'Seatrac' miniature acoustic modem and USBL positioning units for sub-sea robotics and diver applications," in *Proc. IEEE OCEANS*, May 2015, pp. 1–8.
- [34] M. Haenggi, J. G. Andrews, F. Baccelli, O. Dousse, and M. Franceschetti, "Stochastic geometry and random graphs for the analysis and design of wireless networks," *IEEE J. Sel. Areas Commun.*, vol. 27, no. 7, pp. 1029–1046, Sep. 2012.
- [35] M. B. Porter, P. Hurksy, and M. Siderius, "Channel simulation for predicting acoustic modem performance," *J. Acoust. Soc. Amer.*, vol. 125, no. 4, p. 2579, 2009.
- [36] EvoLogics. (Aug. 2017). *Underwater Acoustic Modems Product Information Guide*. [Online]. Available: [https://www.evologics.de/files/DataSheets/EvoLogics\\_S2CR\\_Modems\\_a4\\_WEB.pdf](https://www.evologics.de/files/DataSheets/EvoLogics_S2CR_Modems_a4_WEB.pdf)



**NILS MOROZS** (S'13–M'17) received the M.Eng. and Ph.D. degrees in electronic engineering from the University of York, in 2012 and 2015, respectively. His Ph.D. research was part of the EU FP7 ABSOLUTE project concerned with developing LTE-compliant dynamic spectrum access methods for disaster relief and temporary event networks. He was a Researcher in Wi-Fi and wireless convergence at BT, Martlesham, U.K. He is currently Research Associate at the Department of Electronic Engineering, University of York, where he is involved in channel modelling and medium access control for underwater acoustic sensor networks as part of the EPSRC USMART project. His research interests include the development of protocols and architectures for wireless radio and acoustic networks.



**PAUL MITCHELL** (M'00–SM'09) received the M.Eng. and Ph.D. degrees from the University of York in 1999 and 2003, respectively. His Ph.D. research was on medium access control for satellite systems, which was supported by British Telecom. He has been a member of the Department of Electronic Engineering at University of York since 2002, and is currently a Senior Lecturer. He has gained industrial experience at BT and QinetiQ. He is currently a Lead Investigator on EPSRC USMART (EP/P017975/1) and a Co-Investigator of H2020 MCSA 5G-AURA. He is an author of over 100 refereed journal and conference papers and has served on numerous international conference programme committees. His current research interests include medium access control and networking for underwater and mobile communication systems, and the application of artificial intelligence techniques to such problems. He is a member of the IET and a fellow of the Higher Education Academy. He is an Associate Editor of the *IET Wireless Sensor Systems* journal and the *International Journal of Distributed Sensor Networks* (SAGE). He was the General Chair of the International Symposium on Wireless Communications Systems which was held in York in 2010, and a Track Chair for IEEE VTC in 2015.



**YURIY V. ZAKHAROV** (M'01–SM'08) received the M.Sc. and Ph.D. degrees in electrical engineering from the Power Engineering Institute, Moscow, Russia, in 1977 and 1983, respectively. From 1977 to 1983, he was with the Special Design Agency, Moscow Power Engineering Institute. From 1983 to 1999, he was with the N. N. Andreev Acoustics Institute, Moscow. From 1994 to 1999, he was with Nortel as a DSP Group Leader. Since 1999, he has been with the Communications Research Group, University of York, U.K., where he is currently a Reader in the Department of Electronic Engineering. His research interests include signal processing, communications, and acoustics.

• • •